Enhancement of magnetodielectric coupling in 6H-perovskites $Ba_3RRu_2O_9$ for heavier rare-earth cations ($R = Ho, Tb$)

Tathamay Basu [1,2,3,*] Vincent Caignaert,[1] Somnath Ghara,[3] Xianglin Ke,[2] Alain Pautrat,[1]
Stephan Krohns [3] Alois Loidl [3] and Bernard Raveau[1]

[1]*Laboratoire CRISMAT, UMR 6508 du CNRS et de l'Ensicaen, 6 Boulevard Marechal Juin, 14050 Caen, France*
[2]*Department of Physics and Astronomy, Michigan State University, East Lansing, Michigan 48824, USA*
[3]*Experimental Physics V, Center for Electronic Correlations and Magnetism, University of Augsburg,
Universitätsstrasse 2, D-86135 Augsburg, Germany*

The role of rare-earth (R) ions in magnetodielectric (MD) coupling is always intriguing and markedly different for different systems. Although many reports are available concerning this aspect in frustrated $3d$-transition metal oxides, no such reports exist on higher d ($4d/5d$)-orbital based systems due to the rare availability of highly insulating $4d/5d$ systems. Here, we systematically investigated the magnetic, dielectric, ferroelectric, and magnetodielectric behavior of the 6H-perovskites $Ba_3RRu_2O_9$ for different R-ions, namely $R = Sm$, Tb, and Ho, which magnetically order at 12, 9.5, and 10.2 K, respectively. For $R = Tb$ and Ho, the temperature- and magnetic-field-dependent complex dielectric constant traces the magnetic features, which manifests MD coupling in this system. A weak magnetic-field (H) induced transition is observed for ∼30 kOe, which is clearly captured in H-dependent dielectric measurements. No MD coupling is observed for $Ba_3SmRu_2O_9$. The MD coupling is enhanced by a factor of 3 and 20 times for $R = Tb$ and Ho, respectively, when compared to that of the Nd-counterpart. These results evidence the gradual enhancement of MD coupling with the introduction of heavier R-ions in this series, which is attributed to their larger moment values. Our investigation establishes dominating $4d(Ru)-4f(R)$ magnetic correlation in this series for the heavier R-members.

I. INTRODUCTION

The coexistence of ordered magnetic and lattice degrees of freedom and the cross-coupling between them have been attracting intense attention due to the fundamental scientific interest and promising applications in future storage devices [1–3]. Since the discovery of magnetism-induced ferroelectricity in TbMnO₃ [4], it has been found that many frustrated magnetic systems, containing $3d$-metal-ions and R-ions, exhibit multiferroicity and spin-dipole coupling [1,5,6]. In all these systems, both R-ions (f-orbital) and transition metals (d-orbital) play an important role in establishing magnetism and concomitant magnetoelectric (ME)/magnetodielectric (MD) coupling. The exact role of R-ions in ferroelectricity and ME/MD coupling has not been finally clarified and is still a matter of debate. In general, the ME coupling strength should directly depend on the strength of the polarization, magnetization, and the coupling constant of that system associated with different mechanisms. The different size of R-ions (lanthanide contraction) may play a decisive role in lattice distortion (bond length, angles, etc.) of the system, thereby directly affecting dielectric properties. Further, different radii of R-ions (different degrees of localization/hybridization) and the large magnetic moments of R-ions should have an effect on the overall magnetic structure [e.g., a

change in the exchange interactions and/or heavy moment of R-ions could affect the canting angle of the magnetic moment of a transition metal (TM) ion].

It has been demonstrated that the interactions between the $3d$ and $4f$ electrons of the TM and R sites, respectively, have an important role in their magnetism and magnetoelectric coupling. This is exemplified by the multiferroic RMnO₃ perovskites where the size of the R-ion directly affects the Mn-O-Mn angle and thereby modulates the magnetic structure [7]. For orthorhombic (distorted perovskites) RMnO₃ ($R = $ Eu, Gd, Tb, and Dy), an incommensurate cycloidal magnetic structure of Mn is observed, which breaks the inversion symmetry [as a result of asymmetric Dzyaloshinskii-Moriya (DM) interaction] and drives ferroelectric polarization [8]. A giant MD coupling is observed in DyMnO₃ and GdMnO₃ compared to other R-members [8]. The effect of symmetric exchange-striction, in addition to asymmetric DM interaction, is reported for $R = $ Gd and Dy members in this series [9]. Further heavy rare-earth members crystallize in a hexagonal structure (e.g., HoMnO₃) and exhibit commensurate antiferromagnetic (AFM) ordering. The ferroelectricity in the hexagonal HoMnO₃ oxide arises as a result of displacements of Ho-ions and a possible tilting of MnO₅ polyhedra, and the magnetic structure is not directly involved to create ferroelectricity [10,11]. The MD coupling in this hexagonal system originates from magnetoelastic coupling, where magnetostriction plays an important role. RMn₂O₅ oxides constitute a second example of multiferroic materials,

_____
*tathamaybasu@gmail.com

whose magnetoelectric properties are governed by $3d$-$4f$ electron interactions [12–16]. In RMn$_2$O$_5$, the presence of loops of 5 manganese MnO$_5$/MnO$_6$ polyhedra sharing corners and edges (Mn^{3+}-Mn^{4+}- Mn^{3+}-Mn^{4+}-Mn^{3+}) gives rise to magnetic frustration. It is considered that the symmetric exchange-striction arising from this frustrated structure creates off-centering of an Mn^{+3}-ion, with R ($4f$)–Mn ($3d$) coupling playing an important role in this exchange interaction. The ME coupling is stronger for DyMn$_2$O$_5$ compared to that of TbMn$_2$O$_5$, whereas TbMn$_2$O$_5$ exhibits a switching of polarization in low magnetic fields [12,14]. Interestingly, GdMn$_2$O$_5$ exhibits high polarization and ME coupling compared to all other R-members in this series [15]. The investigation of the light rare-earth (R = Pr, Nd) members reveals weak ME coupling compared to the heavy R-members [16]. Another series of RCrTiO$_5$, derived from the similar RMn$_2$O$_5$ structure, also exhibits multiferroicity and ME coupling, though the role of an R-ion in this series is different from that in RMn$_2$O$_5$ [17–19]. The ME coupling of NdCrTiO$_5$ is stronger than that of GdCrTiO$_5$ [17,19], unlike the ME effect characteristics for the RMn$_2$O$_5$ series. The Haldane-chain oxides, R_2BaNiO$_5$, form another family, where strong $3d$-$4f$ correlation exists via Ni-O-R-O-Ni superexchange paths, and recently they have received considerable attention with respect to multiferroicity and ME coupling [20–25]. In this series, magnetism-induced ferroelectricity with strong ME coupling is proposed for Dy$_2$BaNiO$_5$ [21], whereas ferroelectricity is observed at temperatures well above long-range ordering for many other members (R = Ho, Er, etc.) [20,22]. The light rare-earth Nd member does not exhibit ferroelectricity or ME coupling [26]. A displacement-type ferroelectricity (from NiO$_6$ distortion in an Ni spin-chain) is proposed for the compound Er$_2$BaNiO$_5$ [22]. Interestingly, the compound Tb$_2$BaNiO$_5$ exhibits a giant MD coupling [24], where it is reported that DM interaction between two different magnetic ions (Tb and Ni) is responsible for ferroelectricity, suggesting the influence of strong R ($4f$)−Ni ($3d$) magnetic correlations on ferroelectricity and ME coupling [25]. Therefore, it is quite clear that $3d$-$4f$ interaction is complex depending on the R-ion (different size of the $4f$-orbital and magnetic moment) and it behaves completely differently in various systems.

Up to now, research on multiferroicity/ME coupling in oxides has been mainly restricted to $3d$-TM cations. In the past decade, there has been tremendous interest in $4d$ or $5d$ TM oxides due to their exotic magnetic behavior, arising from the extended electronic orbitals, crystal-field effects, and strong spin-orbit coupling, such as Mott or topological insulating behavior, a quantum spin-liquid state, unconventional superconductivity, or field-driven insulator-metal transitions (for instance, see [27–34] and references therein). However, there are only very few studies of MD coupling in compounds containing a higher d-orbital of ($4d$/$5d$) TM-ions and $4f$-orbital R ions, despite the high interest from theory [35]. Although the larger extension of the $4d$ or $5d$ TM orbitals should favor stronger interactions with the $4f$-R orbitals, it also induces larger overlapping of $4d$-$4d$ (or $5d$-$5d$) orbitals via oxygen, and consequently the investigation of such systems is often experimentally hindered due to the leaky nature (less insulating) of the compounds. Recently, we have reported MD coupling in Ba$_3$NdRu$_2$O$_9$, suggesting interactions between
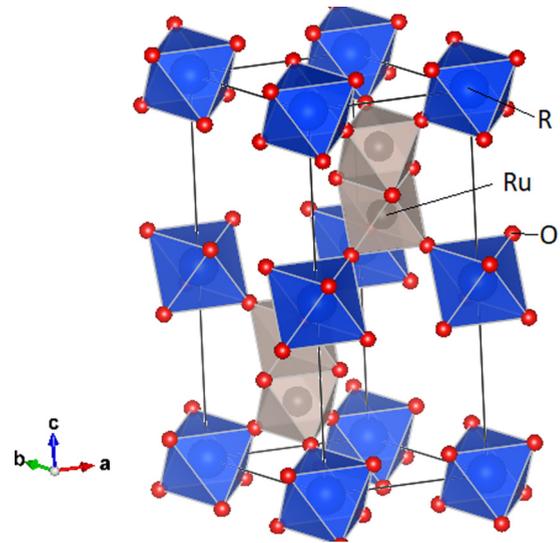
FIG. 1. Crystal structure of Ba$_3$$RRu_2O_9$. For clarity, the Ba atoms are not shown. Two face-sharing distorted RuO$_6$ octahedra (forming a Ru$_2$O$_9$ dimer) and corner-sharing RO$_6$ octahedra are shown.

Ru-$4d$ orbitals and R-$4f$ orbitals, which is a rare demonstration of MD coupling of a $4d$-orbital based magnetic system [36]. We indicate that such properties are made possible by the particular 6H perovskite structure of the Ba$_3$$RRu_2O_9$ oxides (Fig. 1) [37–40], which consists of isolated Ru$_2$O$_9$ dimers of two face-sharing RuO$_6$ octahedra interconnected through RO$_6$ octahedra, in this way hindering electronic delocalization in the whole framework.

Considering the significant effects of R ions on the complex magnetic ordering and ME/MD couplings previously discovered for $3d$ transition-metal based compounds, it is of high interest to investigate the effect of an R-ion ($4f$ orbital) on MD/ME coupling in the Ba$_3$$RRu_2O_9$ $4d$-orbital based system. In fact, the MD coupling in Ba$_3$NdRu$_2$O$_9$ is rather complex and controlled by two different mechanisms, below two magnetic anomalies, at 25 K (ferromagnetic ordering of Nd moments) and 17 K (antiferromagnetic ordering of Nd moments and Ru$_2$O$_9$ dimers), respectively [36,41]. Motivated by this observation, we have investigated three other members of the Ba$_3$$RRu_2O_9$ series with R = Ho, Tb, and Sm. These R-ions are selectively chosen from lanthanide series with respect to ionic radii, valence states, and magnetic moments (see Table I), bearing in mind that in those oxides, Ho/Sm are trivalent and Tb is tetravalent, such that the ruthenium dimers have mixed valence Ru^{4+}/Ru^{5+} and single valence Ru^{4+} states, respectively [37–40]. Unlike the aforementioned Nd-based compound, all three of these compounds exhibit a single magnetic anomaly around 10–12 K [37–41].

II. EXPERIMENTAL DETAILS

The series of oxides Ba$_3$$RRu_2O_9$ was synthesized by solid-state reaction using mixtures of high-purity (>99.9%) precursors BaCO$_3$, RuO$_2$, and R$_2$O$_3$ for R = Ho and Sm and Tb$_4$O$_7$ for R = Tb. These samples were prepared in the form of pellets from intimately mixed powders heated and

TABLE I. Valence state, ionic radius, spin and orbital moments, and magnetic ordering temperatures T_c for different R-ions of the series $Ba_3RRu_2O_9$.

Lanthanide (R) ions and valence states	Ionic radius (pm)	F configurations and effective spin and orbital moments of R-ions	Effective moment of R ($g_J[J(J+1)]^{0.5}$) (μ_B)	T_c/T_N
Ce^{+4}	101	f^0, $S = 0$	0	No
Pr^{+4}	99	f^1, $S = 1/2$, $J = 5/2$	2.54	10.5 K
Nd^{+3}	112.3	f^3, $S = 3/2$, $J = 9/2$	3.62	25 and 17 K
Sm^{+3}	109.8	f^5, $S = 5/2$, $J = 5/2$	0.845	~11 K
Eu^{+3}	108.7	f^6, $S = 3$, $J = 0$	0	~8 K
Gd^{+3}	107.8	f^7, $S = 7/2$, $J = 7/2$	7.94	14.8 K
Tb^{+4}	106.3	f^7, $S = 7/2$, $J = 7/2$	7.94	9.5 K
Ho^{+3}	104.1	f^{10}, $S = 2$, $J = 8$	10.6	10.2 K
Er^{+3}	103	f^{11}, $S = 3/2$, $J = 15/2$	9.6	6 K
Yb^{+3}	100.8	f^{13}, $S = 1/2$, $J = 7/2$	4.54	4.5 K

sintered at temperatures ranging from 1173 to 1573 K with several intermediate grindings, as reported earlier [37–39,42]. The thus grown samples form a single phase with the expected $P6_3/mmc$ space group in agreement with previous literature [37–39,42]. dc magnetization (M) measurements were performed using a Superconducting Quantum Interference Device (SQUID, Quantum Design) as a function of temperature (T) and magnetic field (H). Both temperature- and magnetic-field-dependent measurements of the complex dielectric measurements with a 1 V ac bias were carried out using an LCR meter (Agilent 4284A) with a home-made sample probe, which is integrated into the Physical Properties Measurement System (PPMS, Quantum Design). Silver paint was used to make parallel-plate capacitors of the pressed disklike polycrystalline samples (5 mm diameter and 0.7–0.9 mm thickness for different R-members). Positive-up–negative-down (PUND) measurements were performed in a close-loop refrigerator (Janis) using a TF2000 Analyzer equipped with a high-voltage booster (Trek 609C) to check for ferroelectric polarization.

III. RESULTS

A. $Ba_3HoRu_2O_9$

The T-dependence of the dc magnetic susceptibility of this compound as a function of different magnetic fields is shown in Fig. 2(a). For a 100 Oe external field, the dc magnetization increases with decreasing temperature and exhibits a clear peak at $T_N \sim 10.5$ K, indicative of antiferromagnetic (AFM) order, which agrees with the previous report by Doi *et al.* [38]. The magnetization does not change significantly by increasing the applied magnetic field up to 10 kOe. The application of an external magnetic field of 30 kOe shifts the AFM-type peak to lower temperatures (~ 8.8 K), as shown in Fig. 2(a). For even higher magnetic fields of 50 kOe, the AFM peak is suppressed and the magnetization becomes almost constant below ~ 6 K [Fig. 2(a)]. This decrease of the magnetic-ordering temperature on decreasing temperature is consistent with the proposed AFM behavior. However, such a constant $M(T)$ behavior is not a typical characteristic of a pure AFM system. Figure 2(b) shows the isothermal magnetization [$M(H)$] at selected temperatures. The isothermal $M(H)$ curve

below the magnetic ordering temperature (e.g., at 2 and 7 K) exhibits a linear slope below 30 kOe, like a prototype antiferromagnet. For fields from 30 to 40 kOe, a clear change of slope is observed, unlike a typical AFM system. The inset of Fig. 2(a) shows an enlarged plot of $M(H)$ at 2 K, where a weak hysteresis around 30 kOe is observed. The (sudden) increase in magnetization as a function of magnetic field corresponds
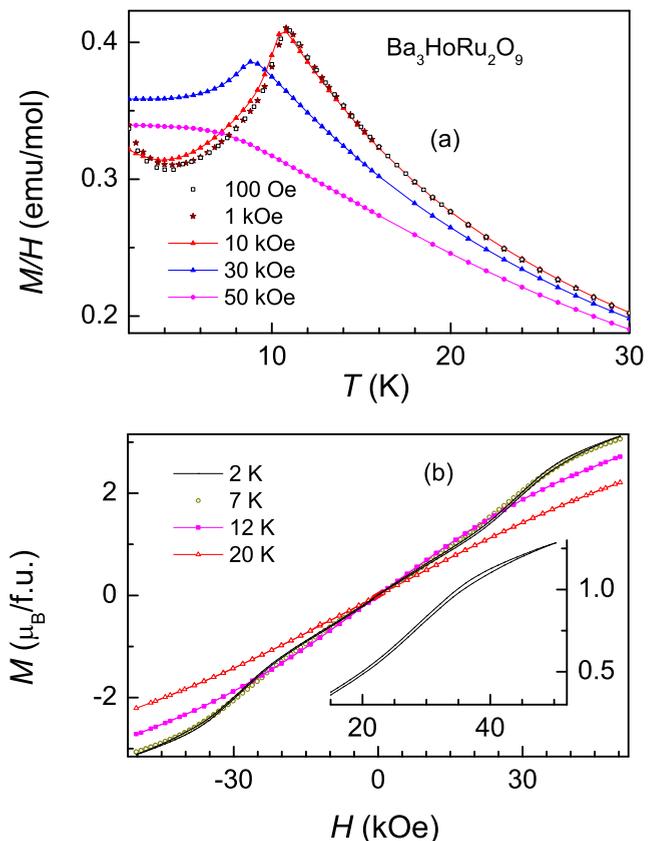
FIG. 2. (a) dc magnetic susceptibility M/H as a function of temperature for a series of magnetic fields ranging from 100 Oe to 50 kOe, and (b) isothermal magnetization M at selected temperatures (2–20 K) for the compound $Ba_3HoRu_2O_9$. The inset shows an enlarged plot of $M(H)$ at 2 K documenting the weak hysteresis.

to an H-induced magnetic transition from AFM behavior. Such a feature might be referred to as meta-magnetic-type transition, keeping in mind that the sharp feature (steplike increase) around the transition is probably smeared out due to its polycrystalline nature. However, further spectroscopic investigation is needed to characterize the exact nature of the magnetic transition and to understand the change in magnetic structure. Possibly, the hysteresis in $M(H)$ at 7 K is not visible due to its very weak nature. The $M(H)$ evolution at $T = 12$ and 20 K is consistent with the paramagnetic nature of this system. Therefore, we conclude that this system undergoes only one AFM ordering transition below T_N, unlike the Nd member in this series. The magnetic behavior as documented in Fig. 2(b) could indicate weak ferromagnetism, such as a canted AFM, or a more complex spin structure due to the presence of competing FM-AFM interactions. Further studies are necessary to elucidate this behavior in full detail. The latter may arise from the ordering of different magnetic ions due to the dominating $4d(\text{Ru}) - 4f(R)$ magnetic correlation compared to the $4d$-$4d$ correlation. Note that we did not observe any further ordering at lower temperatures down to 2 K for the Ho-member. The neutron diffraction on $\text{Ba}_3\text{NdRu}_2\text{O}_9$ shows ferromagnetic ordering of Nd at 24 K and canted AFM ordering of Nd-moments below 18 K with simultaneous ordering of the Ru_2O_9 dimers, where the Nd-moments are aligned along the c-axis with a small tilting toward the ab plane and with Ru-moments aligned within the ab plane [41]. It is not clear whether the ordering at T_N reflects the ordering of the Ho-moments, and the application of high magnetic fields ($H > 30$ kOe) cants the Ho-moments, whereas Ru_2O_9 orders at lower temperature. Another possibility is that both Ru and Ho moments start to order at T_N, the application of magnetic fields further modifies the spin structure, and the system stabilizes in a canted magnetic structure.

Figures 3(a) and 3(b) show the real parts of the dielectric constant (ε') and the loss tangent $\tan\delta$, respectively, as a function of temperature for a fixed frequency of 71.4 kHz in the presence of different magnetic fields. Both ε' and $\tan\delta$ exhibit clear features (kinks and peaks) at the onset of magnetic ordering. No changes in the complex dielectric constant are observed for applied magnetic fields below 10 kOe. As in the magnetic measurements, the observed dielectric feature at T_N shifts to lower temperature for applied magnetic fields <30 kOe and broadens for higher magnetic fields [cf. Figs. 3(a) and 3(b) for $H = 50$ and 90 kOe]. This is in perfect agreement with the results of the magnetic susceptibility, indicating MD coupling. We further confirm this by performing isothermal dielectric measurements (excess dielectric constant, $\Delta\varepsilon' = [\varepsilon'(H) - \varepsilon'(0)]/\varepsilon'(0)$), as shown in Fig. 3(c). The magnetic-field-dependent changes, $\Delta\varepsilon'$, remain nearly constant up to ~10 kOe, then quadratically increase with increasing H, and finally exhibit a jump above 30 kOe, mimicking the H-induced change in $M(H)$. A similar H-induced jump in the dielectric constant is observed in many frustrated multiferroic systems as a result of strong MD coupling exactly near the meta-magnetic transition [19,21,43,44]. No hysteresis is observed in $\Delta\varepsilon'(H)$ as it is very weak at 7 K and not even visible in $M(H)$. Obviously, no such feature is observed above T_N. The MD coupling at 7 K ($T < T_N$) is positive, whereas it is negative at 12 K ($T > T_N$), consistent with $\varepsilon'(T)$
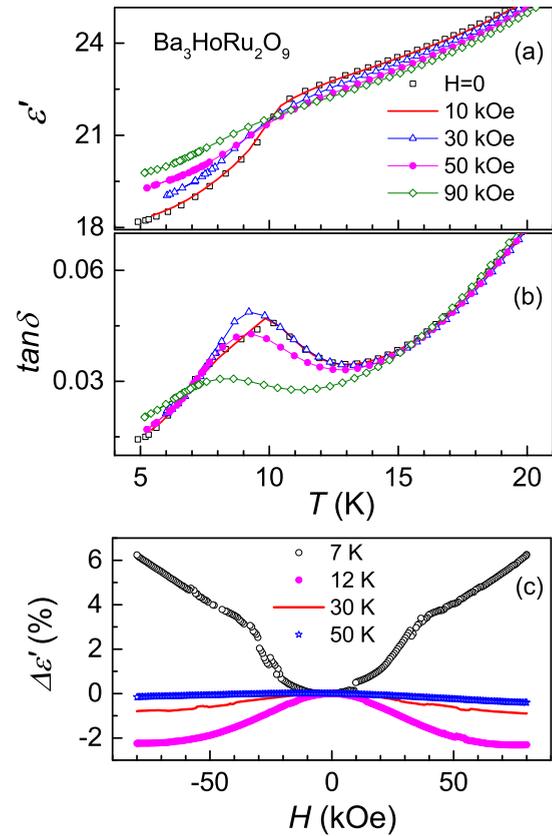
FIG. 3. (a) Real part of the dielectric constant and (b) loss tangent as a function of temperature for different magnetic fields for a fixed frequency of 71.4 kHz for the compound $\text{Ba}_3\text{HoRu}_2\text{O}_9$. (c) The excess dielectric constant $\Delta\varepsilon'(= [\varepsilon'(H) - \varepsilon'(0)]/\varepsilon'(0))$ as a function of magnetic field for 71.4 kHz at selective temperatures.

as a function of increasing external fields. The negative MD coupling decreases with increasing temperature and becomes nearly zero at even higher temperature [see Fig. 3(c)]. The MD effect above magnetic ordering is due to magnetoelastic coupling, which can be observed in the paramagnetic region as well. The system is highly insulating at low temperature, as depicted by the low value of $\tan\delta$; however, it starts to increase sharply above 15 K. Therefore, the absolute value could be magnified by a small leakage contribution at higher temperature, predicted for the compound $\text{Ba}_3\text{NdRu}_2\text{O}_9$ [36].

To check for ferroelectric polarization, we performed nonlinear measurements, i.e., PUND measurements, at 5 K. The sample was cooled down from 50 to 5 K with an applied electrical poling field of 4 kV/cm. At 5 K the poling field was switched off and the sample was kept without any electric fields for 10 min to avoid charging effects. In PUND measurements, two consecutive pulses are used with a time delay between them; application of the first pulse (switching pulse) orients both intrinsic dipoles (if it is ferroelectric) and extrinsic contributions (arising, e.g., from leakage current), which results in changes in output current; when the applied voltage becomes zero, the extrinsic polarization becomes zero; however, dipoles due to intrinsic ferroelectric polarization remain ordered; application of a second pulse (a nonswitching pulse with a similar amplitude, direction,
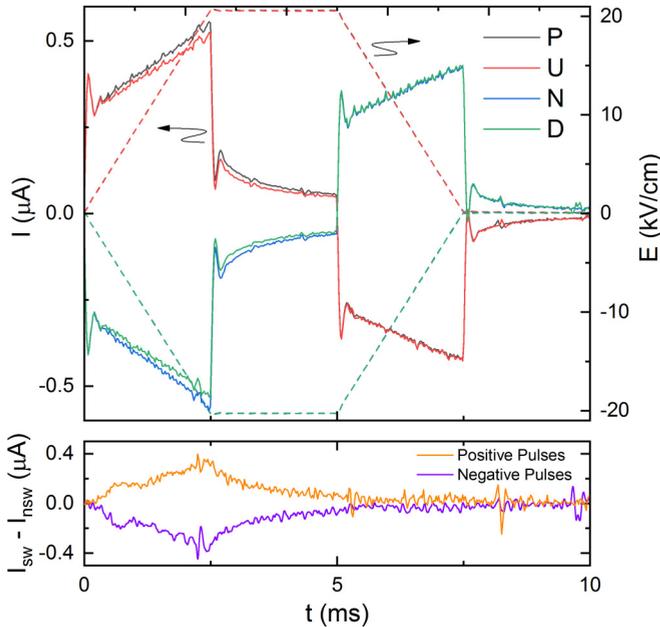
FIG. 4. Results of PUND measurement as discussed in the text. The upper panel shows applied voltage (right axis) and obtained current (left axis) vs pulse time. P and U correspond to two consecutive positive pulses with a 1 s delay, and N and D correspond to two consecutive negative pulses. The lower panel shows the difference in obtained current between P and U positive pulses and N and D negative pulses.

and frequency to those of the first one) again orders the extrinsic dipoles, and the output current arises only from these extrinsic effects; therefore, any difference in current between these two pulses indicates the intrinsic value of polarization. PUND measurement is often better suited to detect small polarizations of a ferroelectric sample excluding all extrinsic effects [45–47]. The result of the PUND measurement, using electrical excitation fields up to 20 kV/cm, does not reveal a typical signature of a proper ferroelectric behavior. However, there are distinct differences between subsequent switching and nonswitching pulses (Fig. 4). From these results, a relaxed remnant polarization in the order of 30 μC/m^2 can be estimated, indicating an unconventional ferroelectric polarization in this system. Reversing the electric field reverses the polarization that confirms ferroelectricity. Although the value of polarization is very small, no such polarization is observed for Nd-members in this series [36].

To find out the role of the *R*-ion, we have pursued MD measurements of the Sm^{3+} member of this series, whose ionic radius falls between Nd^{3+} and Ho^{3+}.

B. Ba$_3$SmRu$_2$O$_9$

The compound Ba$_3$SmRu$_2$O$_9$ exhibits a broad anomaly at high temperature (differently from the Nd and Ho members), but (similar to them) it shows long-range magnetic ordering at 12.5 K (T_N) [40]. However, the application of a high magnetic field (up to 50 kOe) does not modify the magnetic nature of this system, as documented in Fig. 5, unlike Nd and Ho oxides in this series. The observed low magnetic moment may be related to several factors. One is due to the low magnetization
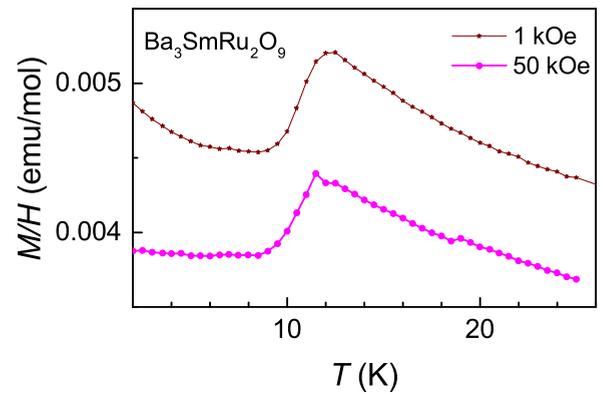
FIG. 5. dc magnetic susceptibility as a function of temperature for 1 and 50 kOe for the Ba$_3$SmRu$_2$O$_9$.

value of Sm^{3+}. The magnetization of the Sm-member certainly is low with respect to the low magnetic moment of Sm^{+3} (Hund's rule) compared to that of other *R*-members in this series (Table I). In addition, the Sm^{3+} magnetic moment is extremely sensitive and may be strongly reduced due to crystal-field effects (e.g., Ref. [48]), compared to the free-ion value given by Hund's rule. Another possibility is that the Sm-moment does not undergo long-range ordering at T_N; the Ru$_2$O$_9$ dimers undergo long-range ordering as observed in the La^{+3}/Pr^{+4} (nonmagnetic)-member of this series. Our results demand further spectroscopic investigation in this respect.

We have investigated the dielectric behavior of this Sm-member. We do not observe any clear dielectric feature at the onset of T_N (not shown here), unlike Nd and Ho members in this series. No MD coupling is observed (see Sec. IV).

In an attempt to understand the role of the oxidation states of both *R* and Ru cations and the effect of magnetic moments of *R*-ions on the magnetodielectric properties of these oxides, we have investigated Ba$_3$TbRu$_2$O$_9$, which exhibits for both cations the tetravalent state, i.e., Tb^{4+} (instead of R^{3+}) and Ru^{4+} (instead of Ru^{4+}/Ru^{5+}), a feature different from other members.

C. Ba$_3$TbRu$_2$O$_9$

The compound Ba$_3$TbRu$_2$O$_9$ orders antiferromagnetically at ∼9.5 K [39], as documented in Fig. 6(a), which was ascribed to antiferromagnetic ordering of the *R*-ions. The ordering temperature decreases with increasing magnetic field, consistent with its AFM nature. Application of a high magnetic field (say, 50 kOe) yields a broad peak, indicating a subtle change in the nature of magnetic ordering. An *H*-induced magnetic transition with a clear magnetic hysteresis at ∼25 kOe in isothermal $M(H)$ below magnetic ordering [see Fig. 6(b)] supports such a change in magnetism. The hysteresis around 25 kOe (and no hysteresis around $H = 0$) for Ba$_3$TbRu$_2$O$_9$ is quite clear compared to that of Ba$_3$HoRu$_2$O$_9$. This often arises as a result of first-order transition, though one cannot rule out the possibility of domain dynamics, specifically in a polycrystalline sample.

Figures 7(a) and 7(b) show $\varepsilon'(T)$ and $\tan\delta(T)$, respectively, measured at 71.4 kHz in zero field and for various applied magnetic fields. The dielectric anomalies (change
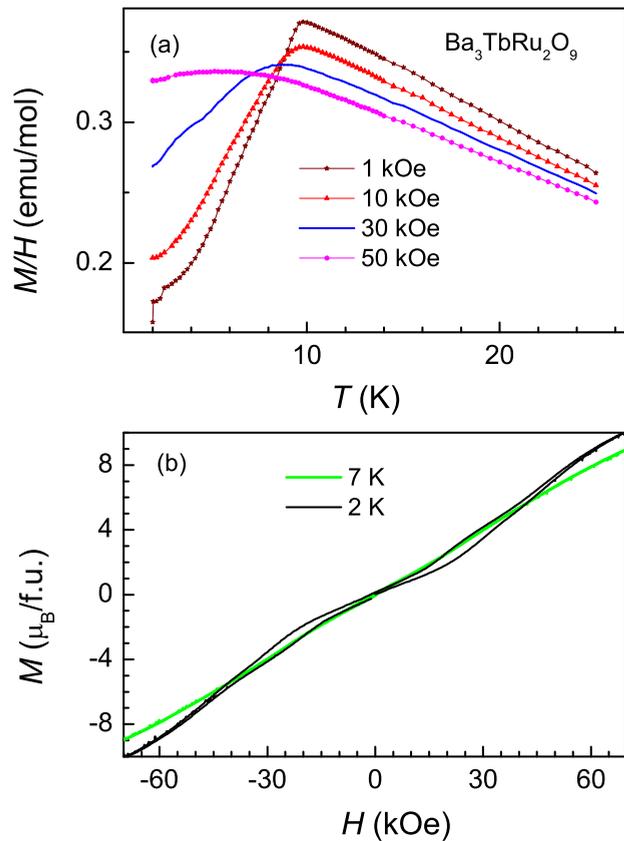
FIG. 6. (a) dc magnetic susceptibility as a function of temperature for different magnetic field (1–50 kOe) and (b) isothermal magnetization at 2 and 7 K for $Ba_3TbRu_2O_9$.

FIG. 7. (a) Real part of the dielectric constant and (b) loss tangent as a function of temperature for different magnetic fields for a fixed frequency of 71.4 kHz for the compound $Ba_3TbRu_2O_9$. (c) The excess dielectric constant $\Delta\varepsilon'(= [\varepsilon'(H) - \varepsilon'(0)]/\varepsilon'(0))$ as a function of magnetic fields measured at 71.4 kHz at selective temperatures for $Ba_3TbRu_2O_9$.

in slope in ε' and the peak in $\tan\delta$) capture the magnetic ordering around 10 K in zero magnetic field, which is continuously shifted to low temperatures with increasing magnetic fields [i.e., from 9.5 K ($H = 0$) to 6.5 K ($H = 50$ kOe)] and becomes fully suppressed by an applied magnetic field of 90 kOe. At 7 K, the excess dielectric constant $\Delta\varepsilon'(H)$ [Fig. 7(c)] exhibits an H-induced transition around 25 kOe, as observed in $M(H)$, which sharply increases above 30 kOe with increasing H. A small MD coupling is observed above the ordering temperature [Fig. 7(c) for $T = 12$ and 30 K], which is consistent with the behavior of $\varepsilon'(T)$ in Figs. 7(a) and 7(b). Such a small MD coupling may arise from short-range magnetic correlations.

IV. DISCUSSION AND CONCLUSION

This study shows that the $R =$ Ho and Tb oxides exhibit MD coupling similar to what was previously observed for the $R =$ Nd oxide [36]. Importantly, the magnitude of this effect is strongly enhanced, namely by a factor of 3 and 20 for Tb and Ho, respectively, as illustrated from the evolution of the excess dielectric constant versus magnetic field at 7 K (Fig. 8). Such behavior is closely related to the appearance of an AFM (or canted AFM) transition at 18, 12, and 10 K for Nd, Ho, and Tb oxides, respectively. For the Nd compound, the magnetic ordering below 18 K originates from an AFM

FIG. 8. The excess dielectric constant $\Delta\varepsilon'$ as a function of magnetic field for 71.4 kHz at 7 K for $R =$ Nd, Sm, Tb, and Ho in the series $Ba_3RRu_2O_9$. The inset shows the same plot for the Nd and Sm members for better visibility of the MD coupling in these compounds.

ordering of Ru-Ru FM dimers and canted AFM ordering of Nd [41]. Thus, our study suggests that the MD coupling in those oxides results from the combination of superexchange AFM interactions between RO$_6$ octahedra and RuO$_6$ with direct FM interactions between the Ru atoms of the Ru$_2$O$_9$ dimers according to the sequence "R-O-Ru-Ru-O-R." Within this model, one would expect that the $R =$ Sm oxide, which exhibits a T_N of 12 K intermediate between the Nd and Ho phases, should also exhibit a MD coupling. This is in contrast with our observation (see Fig. 8). However, the lanthanide contraction (size effect) is not the only parameter that would account for the MD coupling. In particular, the weak magnetic moment of Sm^{3+}(0.845 μ_B) compared to other cations Nd^{3+}(3.62 μ_B), Ho^{3+}(10.6 μ_B), and Tb^{4+}(7.94 μ_B) may explain that for the Sm oxide. The increasing value of $\Delta\varepsilon'(H)$ with the magnetic moment following the sequence Sm < Nd < Tb < Ho strongly supports this hypothesis. Such a systematic increase of MD coupling with R-ion, characteristic of a systematic increase of the R-moments, is a rare observation in this field. It is difficult to explain the exact mechanism of MD coupling in this 6H-perovskite system without any detailed spectroscopic investigation. The canted antiferromagnetic structure is reported for Nd members in this series, where the possible role of DM interaction on positive MD coupling at low temperature is speculated, in addition to a possible magnetostriction effect. No such canted AFM behavior in zero magnetic field is reported for other members of this system, though our detailed magnetic results suggest a possible canting above the H-induced magnetic transition for $R =$ Tb and Ho. Therefore, DM interaction from the canted magnetic structure (in the presence of a high magnetic field at least) probably plays an important role in inducing strong MD coupling. The magnetic exchange energy should be influenced by different extension of rare-earth ions. Interestingly, the magnetic ordering temperature of a light rare-earth (Nd) member is more than two times higher than that of heavy rare-earth members, in contrast with de Gennes scaling [49]. In addition, Ba$_3$NdRu$_2$O$_9$ orders ferromagnetically whereas all other rare-earth members order antiferromagnetically. This kind of unusual nature of magnetic ordering for light rare-earth (Nd) compared to that of heavy rare-earths was often attributed to 4f-hybridization in intermetallic systems (such as R_2PdSi$_3$; see Ref. [50]). However, such 4f-hybridization is probably difficult to posturize in these highly insulating materials. Magnetic frustration, i.e., exchange frustration due to competing interactions between Ru and R-moments, in this complex system could play a significant role in the magnetism and thereby MD coupling. It should be noted that the R-moments are almost aligned parallel to the c-axis whereas the Ru-moments are aligned within the ab plane at low temperatures (assuming Ba$_3$NdRu$_2$O$_9$ magnetic structure [41]). Therefore, magnetic frustration will be strongly influenced by 4d-4f magnetic correlations. The strength of magnetic moments and different degrees of hybridization of different R-ions will both

play a significant role in such strong correlations. It is possible that the stronger magnetic moments of the heavy rare-earths (Ho > Tb > Nd) increase this exchange frustration (due to competing moments of R and Ru). Therefore, heavier rare-earth members undergo long-range ordering at even lower temperature compared to that of their Nd-counterparts by minimizing the frustration. This could be consequential to a larger lattice distortion as well to minimize the overall energy, which yields a dielectric anomaly at magnetic ordering and strong MD coupling. A weak ferroelectricity is confirmed via PUND measurements for Ho-members in this series, although the absolute value of polarization is very small. However, no signature of ferroelectricity is obtained for a light rare-earth Nd member. This further supports our conclusion. It is possible that this system is multiferroic-I with a very small polarization value, where the strong spin-dipole coupling below magnetic ordering arises from a higher-order coupling term instead of linear magnetoelectric coupling. Such a dominant effect of the higher-order coupling term below magnetic ordering is demonstrated in the hexagonal multiferroic RMnO$_3$ [10,11]. One cannot rule out the small effect of magnetostriction due to a change in lattice parameter (an artifact of the geometrical effect of a capacitor). However, this effect cannot be solely responsible for a large MD coupling (say, for an Ho-member, see Fig. 8) since such a huge change in lattice parameter is unlikely (no structural change is observed at the onset of magnetic ordering).

In summary, we have performed a detailed study of both the magnetic and magnetodielectric behavior of Ba$_3$$RRu_2O_9$ oxides for different rare-earth members, selectively chosen from the broad series. A strong enhancement of MD coupling, 3 and 20 times, is demonstrated for heavy rare-earth members Tb and Ho, respectively, compared to the Nd one, which is independent of the valence state of the R and Ru cations. In contrast, no MD coupling is observed for the Sm-phase in spite of the size of Sm^{3+} intermediate between Nd^{3+} and Ho^{3+}. This feature suggests that the strength of MD coupling in this system is mainly governed by two parameters that may be antagonist, the size (lanthanide contraction), and the magnetic moment of the rare earth. A detailed neutron investigation on different R-members is warranted in order to underpin the exact nature of d-f correlation and the mechanism of MD coupling.

[1] Y. Tokura, S. Seki, and N. Nagaosa, Rep. Prog. Phys. **77**, 076501 (2014).

[2] M. Bibes and A. Barthélémy, Nat. Mater. **7**, 425 (2008).

[3] Y. Tokunaga, N. Furukawa, H. Sakai, Y. Taguchi, T. Arima, and Y. Tokura, Nat. Mater. **8**, 558 (2009).

[4] T. Kimura, T. Goto, H. Shintani, K. Ishizaka, T. Arima, and Y. Tokura, Nature (London) **426**, 55 (2003).

[5] S. J. Yuan, W. Ren, F. Hong, Y. B. Wang, J. C. Zhang, L. Bellaiche, S. X. Cao, and G. Cao, Phys. Rev. B **87**, 184405 (2013).

[6] A. K. Zvezdin and A. A. Mukhin, JETP Lett. **88**, 505 (2008).

[7] N. Aliouane, O. Prokhnenko, R. Feyerherm, M. Mostovoy, J. Strempfer, K. Habicht, K. C. Rule, E. Dudzik, A. U. B. Wolter, A. Maljuk, and D. N. Argyriou, J. Phys.: Condens. Matter **20**, 434215 (2008).

[8] T. Goto, T. Kimura, G. Lawes, A. P. Ramirez, and Y. Tokura, Phys. Rev. Lett. **92**, 257201 (2004).

[9] R. Feyerherm, E. Dudzik, O. Prokhnenko, and D. N. Argyriou, J. Phys.: Conf. Ser. **200**, 012032 (2010).

[10] N. Hur, I. K. Jeong, M. F. Hundley, S. B. Kim, and S.-W. Cheong, Phys. Rev. B **79**, 134120 (2009).

[11] J. Liu, Y. Gallais, M.-A. Measson, A. Sacuto, S. W. Cheong, and M. Cazayous, Phys. Rev. B **95**, 195104 (2017).

[12] N. Hur, S. Park, P. A. Sharma, J. S. Ahn, S. Guha, and S.-W. Cheong, Nature (London) **429**, 392 (2004).

[13] S. H. Bukhari, Th. Kain, M. Schiebl, A. Shuvaev, A. Pimenov, A. M. Kuzmenko, X. Wang, S.-W. Cheong, J. Ahmad, and A. Pimenov, Phys. Rev. B **94**, 174446 (2016).

[14] N. Hur, S. Park, P. A. Sharma, S. Guha, and S.-W. Cheong, Phys. Rev. Lett. **93**, 107207 (2004).

[15] N. Lee, C. Vecchini, Y. J. Choi, L. C. Chapon, A. Bombardi, P. G. Radaelli, and S.-W. Cheong, Phys. Rev. Lett. **110**, 137203 (2013).

[16] S. Chattopadhyay, V. Balédent, F. Damay, A. Gukasov, E. Moshopoulou, P. Auban-Senzier, C. Pasquier, G. André, F. Porcher, E. Elkaim, C. Doubrovsky, M. Greenblatt, and P. Foury-Leylekian, Phys. Rev. B **93**, 104406 (2016).

[17] J. Hwang, E. S. Choi, H. D. Zhou, J. Lu, and P. Schlottmann, Phys. Rev. B **85**, 024415 (2012).

[18] T. Basu, K. Singh, S. Gohil, S. Ghosh, and E. V. Sampathkumaran, J. Appl. Phys. **118**, 234103 (2015).

[19] T. Basu, D. T. Adroja, F. Kolb, H.-A. Krug von Nidda, A. Ruff, M. Hemmida, A. D. Hillier, M. Telling, E. V. Sampathkumaran, A. Loidl, and S. Krohns, Phys. Rev. B **96**, 184431 (2017).

[20] G. Nénert and T. T. M. Palstra, Phys. Rev. B **76**, 024415 (2007).

[21] K. Singh, T. Basu, S. Chowki, N. Mahapotra, K. K. Iyer, P. L. Paulose, and E. V. Sampathkumaran, Phys. Rev. B **88**, 094438 (2013).

[22] T. Basu, V. V. R. Kishore, S. Gohil, K. Singh, N. Mohapatra, S. Bhattacharjee, B. Gonde, N. P. Lalla, P. Mahadevan, S. Ghosh, and E. V. Sampathkumaran, Sci. Rep. **4**, 5636 (2014).

[23] S. Chowki, T. Basu, K. Singh, N. Mohapatra, and E. V. Sampathkumaran, J. Appl. Phys. **115**, 214107 (2014).

[24] S. K. Upadhyay, P. L. Paulose, and E. V. Sampathkumaran, Phys. Rev. B **96**, 014418 (2017).

[25] R. Kumar, S. Rayaprol, S. Rajput, T. Maitra, D. T. Adroja, K. K. Iyer, S. K. Upadhyay, and E. V. Sampathkumaran, Phys. Rev. B **99**, 100406(R) (2019).

[26] T. Basu, N. Mohapatra, K. Singh, and E. V. Sampathkumaran, AIP Adv. **5**, 037128 (2015).

[27] J. G. Rau, E. K.-H. Lee, and H.-Y. Kee, Annu. Rev. Condens. Matter Phys. **7**, 195 (2016).

[28] A. Akbari and G. Khaliullin, Phys. Rev. B **90**, 035137 (2014).

[29] T. Dey, A. V. Mahajan, P. Khuntia, M. Baenitz, B. Koteswararao, and F. C. Chou, Phys. Rev. B **86**, 140405(R) (2012).

[30] B. J. Kim, H. Ohsumi, T. Komesu, S. Sakai, T. Morita, H. Takagi, and T. Arima, Science **323**, 1329 (2009).

[31] Y. Singh and P. Gegenwart, Phys. Rev. B **82**, 064412 (2010).

[32] A. P. Mackenzie and Y. Maeno, Rev. Mod. Phys. **75**, 657 (2003).

[33] M. Majumder, F. Freund, T. Dey, M. Prinz-Zwick, N. Büttgen, Y. Skourski, A. Jesche, A. A. Tsirlin, and P. Gegenwart, Phys. Rev. Mater. **3**, 074408 (2019).

[34] M. Zhu, J. Peng, T. Zou, K. Prokes, S. D. Mahanti, T. Hong, Z. Q. Mao, G. Q. Liu, and X. Ke, Phys. Rev. Lett. **116**, 216401 (2016).

[35] M. Ležaić and N. A. Spaldin, Phys. Rev. B **83**, 024410 (2011).

[36] T. Basu, A. Pautrat, V. Hardy, A. Loidl, and S. Krohns, Appl. Phys. Lett. **113**, 042902 (2018).

[37] Y. Doi, Y. Hinatsu, Y. Shimojo, and Y. Ishii, J. Solid State Chem. **161**, 113 (2001).

[38] Y. Doi and Y. Hinatsu, J. Mater. Chem. **12**, 1792 (2002).

[39] Y. Doi, M. Wakeshima, Y. Hinatsu, A. Tobo, K. Ohoyama, and Y. Yamaguchi, J. Mater. Chem. **11**, 3135 (2001).

[40] Y. Doi, K. Matsuhira, and Y. Hinatsu, J. Solid State Chem. **165**, 317 (2002).

[41] M. S. Senn, S. A. J. Kimber, A. M. Arevalo Lopez, A. H. Hill, and J. P. Attfield, Phys. Rev. B **87**, 134402 (2013).

[42] Y. Doi, M. Wakeshima, Y. Hinatsu, A. Tobo, K. Ohoyama, and Y. Yamaguchi, J. Alloys Compd. **344**, 166 (2002).

[43] T. Basu, K. K. Iyer, K. Singh, and E. V. Sampathkumaran, Sci. Rep. **3**, 3104 (2013).

[44] T. Basu, C. Bloyet, F. Beaubras, V. Caignaert, O. Perez, J.-M. Rueff, A. Pautrat, B. Raveau, J.-F. Lohier, P.-A. Jaffrès, H. Couthon, G. Rogez, G. Taupier, and H. Dorkenoo, Adv. Funct. Mater. **29**, 1901878 (2019).

[45] J. F. Scott, *Ferroelectric Memories*, Springer Series in Advanced Microelectronics (Springer, Berlin, 2010).

[46] J. F. Scott, J. Phys.: Condens. Matter **20**, 021001 (2008).

[47] A. Loidl, S. Krohns, J. Hemberger, and P. Lunkenheimer, J. Phys.: Condens. Matter **20**, 191001 (2008).

[48] S. K. Malik and R. Vijayaraghavan, Pramana–J. Phys. **3**, 122 (1974).

[49] P.-G. Gennes, *Scaling Concepts in Polymer Physics* (Cornell University Press, Ithaca, NY, 1979).

[50] K. Mukherjee, T. Basu, K. K. Iyer, and E. V. Sampathkumaran, Phys. Rev. B **84**, 184415 (2011).